JBC RESEARCH ARTICLE

Cartwheel disassembly regulated by CDK1-cyclin B kinase allows human centriole disengagement and licensing

Received for publication, February 26, 2022, and in revised form, October 22, 2022 Published, Papers in Press, November 7, 2022,
https://doi.org/10.1016/j.jbc.2022.102658

Fan Huang, Xiaowei Xu, Guangwei Xin, Boyan Zhang, Qing Jiang, and Chuanmao Zhang*

From the Key Laboratory of Cell Proliferation and Differentiation of the Ministry of Education, College of Life Sciences, Peking University, Beijing, China

Edited by Brian Strahl

Cartwheel assembly is considered the first step in the initiation of procentriole biogenesis; however, the reason for persistence of the assembled human cartwheel structure from S phase to late mitosis remains unclear. Here, we demonstrate mainly using cell synchronization, RNA interference, immunofluorescence and time-lapse-microscopy, biochemical analysis, and methods that the cartwheel persistently assembles and maintains centriole engagement and centrosome integrity during S phase to late G2 phase. Blockade of the continuous accumulation of centriolar Sas-6, a major cartwheel protein, after procentriole formation induces premature centriole disengagement and disrupts pericentriolar matrix integrity. Additionally, we determined that during mitosis, CDK1-cyclin B phosphorylates Sas-6 at T495 and S510, disrupting its binding to cartwheel component STIL and pericentriolar component Nedd1 and promoting cartwheel disassembly and centriole disengagement. Perturbation of this phosphorylation maintains the accumulation of centriolar Sas-6 and retains centriole engagement during mitotic exit, which results in the inhibition of centriole reduplication. Collectively, these data demonstrate that persistent cartwheel assembly after procentriole formation maintains centriole engagement and that this configuration is relieved through phosphorylation of Sas-6 by CDK1-cyclin B during mitosis in human cells.

As the major microtubule-organizing center, the centrosome regulates cell polarity, motility, intracellular material transport during interphase, and spindle assembly during mitosis. A mature centrosome comprises two barrel-shaped centrioles surrounded by pericentriolar matrix (PCM) (1–4). The centrosome duplicates once per cell cycle within an accurate duplication cycle, which is controlled by complicated regulatory networks composed of a wide diversity of regulatory proteins and kinases to ensure that centrosome duplication occurs properly (5).

To initiate a centrosome cycle, disengagement of the paired centrioles during mitotic exit is a prerequisite (6, 7). Up to early S phase, each of the disengaged centrioles acts as a mother centriole to initiate cartwheel assembly at its lateral proximal end, followed by microtubule nucleation around the cartwheel for biogenesis of the daughter centriole (8–10). Once generated, the daughter centriole stays well engaged with its mother until their disengagement during the next mitotic exit in order to ensure that centriole duplication occurs once per cell cycle for accurate cell division (5, 6, 10, 11).

Previous studies have identified a conserved mechanism for daughter centriole biogenesis in human cells, in which Polo-like kinase 4 (Plk4) serves as a master regulator and Sas-6 as a key component for initiating the assembly of a cartwheel as a pedestal at the existing lateral site of the mother centriole (12–18). Plk4 is initially recruited to the mother centriole by the PCM scaffold components Cep192 and Cep152 (19–23). More recently, we found that under the regulation of Plk4, Nedd1 is recruited before Sas-6 to the PCM by Cep192 and another PCM scaffold component PCNT, serving as a platform to recruit Sas-6 for cartwheel assembly and centriole biogenesis (24). Plk4 also phosphorylates STIL to facilitate the recruitment of centriolar Sas-6 (25–29). After the initiation of daughter centriole biogenesis has been completed, Sas-6 is continuously recruited and immobilized to the daughter centriole during cell cycle progression from S phase to late G2 phase, leading to an increase in the size of the cartwheel structure (30). The cartwheel is characterized by a central hub from which nine spokes project. Sas-6, in particular, constitutes the primary backbone of the cartwheel, which forms homodimers *via* the coiled-coil domains. Nine adjacent homodimers can self-oligomerize *via* the N-terminal head domain to form a ring resembling the central hub, with the C-erminal tails oriented outward as spokes (31–36). In human cells, the Sas-6-assembled cartwheel is a transient scaffolding structure that is disassembled during procentriole maturation in mitosis (14). More recently, Sas-6 has been shown to stabilize centriole intermediates in early S phase to suppress the formation of extra initiation sites for cartwheel assembly and daughter centriole biogenesis (37). However, both the significance of continuous Sas-6 recruitment and immobilization to the daughter centriole during S phase to late G2 phase and the mechanism responsible for disassembly of the cartwheel during mitosis remain unclear.

Based on our previous research findings that Sas-6 is recruited by Nedd1 under the regulation of Plk4 for the initiation of cartwheel assembly and centriole biogenesis (24), we further explored the role of Sas-6 after the initiation of

* For correspondence: Chuanmao Zhang, zhangcm@pku.edu.cn.

daughter centriole biogenesis has been completed. Here, we demonstrate that Sas-6 plays a crucial role in maintaining the association of paired centrioles until late G2/M phase transition. Subsequently, CDK1-cyclin B kinase phosphorylates Sas-6 at T495 and S510 during mitotic entry, which reduces the binding affinity of Sas-6 for STIL and Nedd1 and promotes the disassociation of Sas-6 from the daughter centriole, leading to cartwheel disassembly and centriole disengagement. Collectively, our data reveal a novel function of the cartwheel and a novel mechanism underlying cartwheel disassembly during mitosis, aiding our understanding of the manner by which the centrosome duplication and cell cycles are coordinated.

Results

Sas-6 accumulation maintains centriole engagement and PCM integrity

Immunostaining of Sas-6 and Centrin1, a known centriole subdistal-end marker, confirmed the centriolar localization of Sas-6 during S phase, G2 phase, and early mitosis in HeLa cells (Fig. S1*A*). Additionally, time-lapse microscopy of stable GFP-Sas-6-expressing HeLa cells showed that after completion of the initiation of daughter centriole biogenesis, the levels of centriolar GFP-Sas-6 increased steadily from S phase to G2/M transition, as previously reported (30) and rapidly decreased from nuclear envelope breakdown to late mitosis (Fig. S1, *B*, *C* and Movie S1).

To investigate the reason for continuous accumulation of centriolar Sas-6 after completion of the initiation of daughter centriole biogenesis, we released G1/S phase-arrested HeLa cells into metaphase by sequential treatment with STLC and MG132 and simultaneously knocked down Sas-6 during this period without affecting the initiation of centriole duplication (Figs. 1, *A*, *B* and S2*A*). We studied the structural features of the centrioles during metaphase by immunostaining of centriolar and PCM marker proteins (PCNT, CDK5RAP2, and γ-tubulin). Approximately 15.3% of metaphase cells treated with Sas-6 siRNA exhibited aberrantly separated centrioles, which was typically accompanied by cracked PCM, whereas only roughly 7.3% of control metaphase cells displayed separated centrioles (**$p < 0.01$) (Fig. 1, *C* and *D*). The premature centriole disengagement phenotype was relatively mild due to limited Sas-6 interference efficiency (∼62%) as a result of time restriction (16 h) during the transition from G1/S phase to metaphase to prevent influence on centriole duplication initiation. We also examined other cartwheel components, STIL and CPAP, and found that cells treated with siRNA targeted toward STIL, but not CPAP, displayed aberrantly separated centrioles, albeit to a lesser extent than that seen following Sas-6 knockdown (Fig. S2, *B*–*D*). This may be attributed to the role of STIL in facilitating the loading of Sas-6 onto the centrioles during cartwheel assembly (25–29, 38–40). These results indicate that knockdown of Sas-6 after daughter centriole formation induces premature centriole disengagement and disrupts PCM integrity, since centriole disengagement and PCM cleavage normally only occur during mitotic exit (41–46).

We further investigated the consequences of premature centriole disengagement and cracked PCM. The majority of Sas-6-knockdown cells which displayed abnormally disengaged centrioles and cracked PCM significantly exhibited metaphase spindle misorientation and multipolar mitotic spindle assembly (Fig. S2, *E*–*H*). Collectively, these results suggest that continuous accumulation and persistence of centriolar Sas-6 after daughter centriole biogenesis maintains the engagement of mother and daughter centrioles and the integrity of the PCM (Fig. 1*E*).

CDK1-cyclin B phosphorylates Sas-6 at T495 and S510 during early mitosis

Next, we investigated the regulatory mechanism for the maintenance of centrosome integrity by Sas-6. First, we examined Sas-6 expression and posttranslational modification in HeLa cells during the cell cycle, revealing that the Sas-6 protein expression level decreased rapidly during mitotic exit (Figs. 2*A* and S3*A*). Interestingly, results of the Phos-tag gel assay show that Sas-6 bands were heavily upshifted in prometaphase, which decreased rapidly during mitotic exit (Figs. 2*A* and S3*A*), indicating that Sas-6 was phosphorylated during mitotic entry. To identify the kinase responsible for Sas-6 phosphorylation, mitotic cells were treated with several mitotic kinase inhibitors: BI2536 for Plk1, RO3306 for CDK1-cyclin B, MLN8237 for Aurora A, AZD1152/ZM447439 for Aurora B, and DMSO as a negative control (Materials and Methods). Inhibition of CDK1-cyclin B with RO3306 significantly reduced the upshifted Sas-6 bands (Fig. 2*B*), suggesting that Sas-6 was phosphorylated by CDK1-cyclin B during early mitosis.

GPS 3.0 (Group-based Prediction System, version 3.0) predicted four potential phosphorylation sites in Sas-6 for CDK1-cyclin B: S111, T495, S510, and S657. Accordingly, we constructed Sas-6 mutants carrying a single or double mutation of these amino acids to alanine, expressed them in HeLa cells, and subjected these cells to Phos-tag gel analysis. The GFP-tagged Sas-6 mutant with a single mutation of T495 or S510, both of which are consistent with the phosphorylation consensus sequence ((S/T*)P or (S/T*)P*X*(K/R)) for CDK1-cyclin B (47) to alanine (T495A or S510A), or with double mutation of these two sites (T495A/S510A, denoted as 2A), displayed significantly reduced upshifted bands (Figs. 2*C* and S3*B*). Mass spectrometry (MS) of GFP-Sas-6 immunoprecipitated from HEK293 cells demonstrates that T495 and S510 were indeed phosphorylated during early mitosis (Fig. S3, *C*–*E*). These two sites are conserved in mammals as shown by multiple sequence alignment (Fig. 2*D*). Moreover, RO3306 treatment of prometaphase cells significantly decreased the number of peptides carrying phosphorylated T495 and S510 residues (Fig. S3*D*). Subsequently, we purified GFP-tagged Sas-6 WT and 2A as well as Nedd1 from HEK293 cells and performed an *in vitro* kinase assay with CDK1-cyclin B in the presence of γ-^{32}P ATP. While Sas-6 WT was phosphorylated by CDK1-cyclin B as compared with the heavily positive reference of Nedd1, the 2A mutant showed significantly less

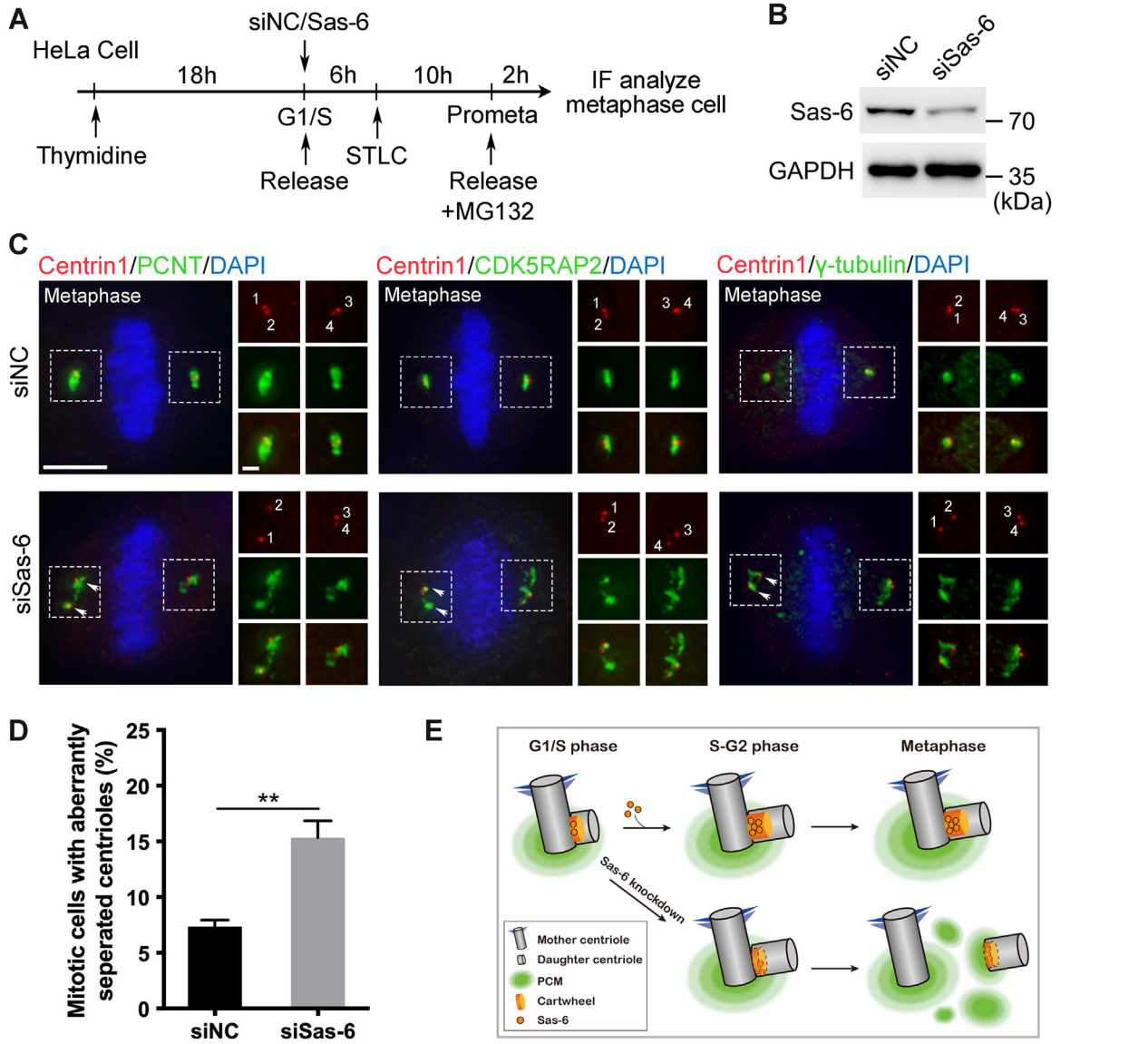

Figure 1. Sas-6 is required for the maintenance of centriole engagement and pericentriolar matrix integrity. *A*, experimental scheme for the generation of mitosis-arrested HeLa cells by Sas-6 knockdown. HeLa cells were arrested at metaphase by sequential treatment with 2.5 μM thymidine, 5 μM STLC, and 10 μM MG132 and simultaneously transfected with Sas-6 siRNA for 18 h. *B*, knockdown efficiency of Sas-6 siRNA. HeLa cells were treated as described in (*A*), harvested, and analyzed by immunoblotting using antibodies against Sas-6 and GAPDH. *C*, Sas-6 knockdown induces abnormal centriole disengagement and disordered pericentriolar matrix (PCM) during mitosis. HeLa cells were treated as described in (*A*), fixed with methanol, and analyzed by immunofluorescence using antibodies against PCNT, CDK5RAP2, γ-tubulin, and Centrin1. DNA was stained with DAPI. *Arrowheads* indicate cracked PCM proteins. The *boxed areas* in each main image are zoomed into the right panels with separated channels. Scale bars, 5 μm (large images) or 1 μm (inset images). *D*, quantitation of the number of cells with aberrantly separated centrioles in (*C*). Centrioles with a distance greater than 1 μm were counted as separated. Approximately 200 cells were counted per sample, and three independent experiments were conducted. The statistical data are expressed as the mean ± SD. $^{**}p < 0.01$ (Student's *t* test). *E*, schematic diagram illustrating that Sas-6 knockdown after daughter centriole assembly induces untimely centriole disengagement and disrupts PCM integrity. See also Figs. S1 and S2.

phosphorylation (Fig. 2*E*). Collectively, we conclude that Sas-6 is phosphorylated by CDK1-cyclin B at T495 and S510 during early mitosis *in vitro* and *in vivo*.

Endogenous pS510-Sas-6 is detectable at centrioles of early mitotic cells

To investigate the spatiotemporal phosphorylation of Sas-6 by CDK1-cyclin B, we raised a phospho-antibody against pS510-Sas-6 by injecting rabbits with a synthetic Sas-6 peptide carrying the phosphorylated S510 residue (506-RSGI(S-p) PNLN-514, denoted phospho-peptide). The specificity of this pS510-Sas-6 antibody was examined and confirmed by immunoblotting (Fig. S4*A*). The pS510-Sas-6 antibody specifically detected Sas-6 in nocodazole-arrested mitotic lysates but not in asynchronized cell lysates. Moreover, following treatment of the mitotic cell lysates with RO3306, but not other kinase inhibitors, the antibody-recognized signal almost disappeared (Fig. S4, *B* and *C*), indicating that Sas-6 was specifically phosphorylated at S510 by CDK1-cyclin B *in vivo* during mitosis. We also confirmed that the pS510-Sas-6 antibody detected GFP-Sas-6 but not GFP-Sas-6-S510A

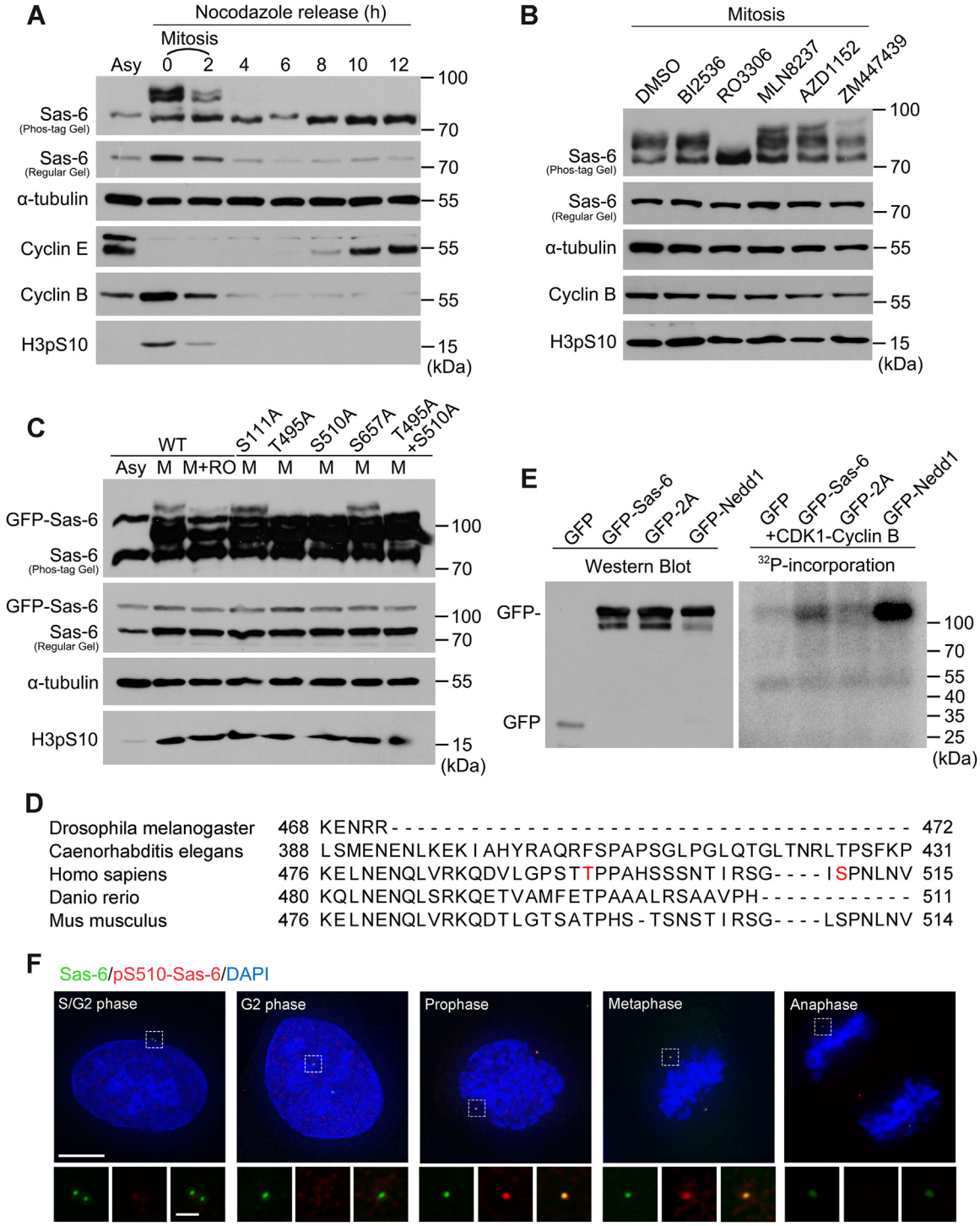

Figure 2. CDK1-cyclin B phosphorylates Sas-6 at T495 and S510 during mitosis. *A*, Sas-6 is phosphorylated during mitosis. HeLa cells were arrested in mitosis by thymidine-nocodazole treatment, released, and harvested at the indicated time points. Asy refers to asynchronized cell samples. Samples were analyzed by immunoblotting using the indicated antibodies. Note the unshifted bands of Sas-6 in mitosis. *B*, Sas-6 is phosphorylated by CDK1-cyclin B during mitosis. Mitosis-arrested HeLa cells were treated with selected kinase inhibitors prior to harvest. Note that treatment with RO3306 for 15 min significantly inhibited the upshift of Sas-6 bands during mitosis. *C*, CDK1-cyclin B phosphorylates Sas-6 at T495 and S510 during mitosis. HeLa cells transfected with GFP-tagged Sas-6 WT and mutants were treated with DMSO or RO3306. M refers to mitotic cell samples, and RO refers to RO3306 treatment. *D*, Sas-6 phosphorylation sites revealed by mass spectrometry, of which two, T495 and S510, are conserved in mammals. Multiple sequence alignment also shows that the Sas-6 phosphorylation sites mediated by CDK1-cyclin B in mammals, as well as the nearby C-terminal sequence, are missing from homologous Sas-6 in *Drosophila*. *E*, CDK1-cyclin B phosphorylates Sas-6 *in vitro*. GFP, GFP-tagged Sas-6, Sas-6 mutant 2A, or Nedd1 proteins purified from HEK293 cells were individually incubated with CDK1-cyclin B in a kinase reaction system, and the incorporation of γ-^{32}P into the substrates was visualized by autoradiography. *F*, endogenous Sas-6 phosphorylated at S510 is detected on centrioles from prophase to metaphase. HeLa cells were fixed with methanol and analyzed by immunofluorescence using antibodies against Sas-6 and pS510-Sas-6. DNA was stained with DAPI. Scale bars, 5 μm (large images) or 1 μm (inset images). See also Figs. S3 and S4.

during mitosis (Fig. S4, *D* and *E*). Immunostaining of HeLa cells demonstrates that pS510-Sas-6 only colocalized with Sas-6 at the centrioles from prophase to metaphase, which is consistent with the active period of CDK1-cyclin B during mitosis (Figs. 2*F*, S4, *F* and *G*). Collectively, these results indicate that CDK1-cyclin B phosphorylates centriolar Sas-6 at S510 during early mitosis.

CDK1-cyclin B promotes centriolar Sas-6 removal to allow centriole disengagement

To investigate the function of centriolar Sas-6 phosphorylation by CDK1-cyclin B, we directly examined the dynamic localization of GFP-Sas-6 on the centrioles during mitosis following treatment of mitotic cells with the CDK1-specific inhibitor RO3306. Consistent with the immunofluorescence and live-cell imaging data (Fig. S1, *A*–*C*), centriolar Sas-6 continuously decreased throughout prophase and metaphase in the DMSO-treated control group and suddenly vanished from anaphase until early G1 phase. By contrast, treatment with RO3306 prevented the removal of Sas-6 from centrioles, with some centriolar Sas-6 remaining with cell cycle progression through mitosis into G1 phase even without proper chromosomal segregation (Fig. 3, *A* and *B*, Movies S2 and S3). This finding indicates that CDK1-cyclin B phosphorylation promotes Sas-6 removal from centrioles during mitosis.

Since Sas-6 is required for the maintenance of centriole engagement and PCM integrity from S phase to late G2 phase (Fig. 1, *C*–*E*), we further investigated whether CDK1-cyclin B–mediated centriolar Sas-6 removal contributes to centriole disengagement during mitotic exit, thus licensing the centriole to duplicate in the next centrosome cycle. Firstly, we synchronized HeLa cells and those stably expressing GFP-Sas-6 in mitosis using the double-thymidine blockade and release approach. Subsequently, mitotic cells were treated with DMSO or RO3306 for 1 h to obtain mitotic exit or early G1 phase cells and subjected to immunofluorescence analysis (Fig. 3*C*). The mitotic exit or early G1 phase synchronization efficiency was determined by two centrioles (two Centrin1 dots), and engagement of the mother/daughter centrioles was determined by a 2:1 ratio of Centrin1 dots to proximal centriole marker C-Nap1 dots. Cells treated with RO3306 were forced into G1 phase with incomplete cytoplasmic division, and the engagement or disengagement configuration within one pair of centrioles was assessed. Immunofluorescence labeling demonstrates that the vast majority of DMSO-treated control cells (∼94.3%) no longer had detectable centriolar Sas-6 and underwent mother/daughter centriole disengagement as expected. On the contrary, approximately 39.7% of RO3306-treated cells steadily maintained centriolar Sas-6, and roughly 28.7% of RO3306-treated cells maintained paired mother/daughter centriole engagement, suggesting that the centrioles carrying Sas-6 during mitotic exit were abnormally engaged (Fig. 3, *D*–*F*). These results indicate that inhibition of the kinase activity of CDK1 prevents Sas-6 removal from the centrioles, resulting in continuous engagement of the mother/daughter centrioles.

To determine the direct function of CDK1-cyclin B–phosphorylated Sas-6, we cotransfected stable RFP-H2B-expressing HeLa cells with Sas-6 3′UTR siRNA and GFP-Sas-6, 2A, or 2D and performed time-lapse microscopy to trace these proteins during mitosis and early G1 phase. The 2A mutant, which is unable to be phosphorylated by CDK1-cyclin B, was prevented from being removed from the centriole, and some 2A remained on the centriole even during late mitosis and early G1 phase. By contrast, WT and 2D rapidly disappeared from the centrioles during late mitosis, although WT remained slightly longer (Fig. 4, *A*–*C* and Movies S4–S6). Collectively, we conclude that CDK1-cyclin B activity is required for centriolar Sas-6 removal and centriole disengagement during mitotic exit in human cells.

Phosphorylation of Sas-6 by CDK1-cyclin B promotes its centriolar disassociation to allow centriole disengagement and licensing

It is known that Sas-6 degradation is targeted by APC/C^{Cdh1} *via* the ubiquitination pathway during late anaphase and G1 phase (14). To distinguish whether CDK1-cyclin B mediated centriolar Sas-6 removal occurs prior to its degradation or is directly dependent on its degradation, we analyzed Sas-6 protein expression levels in mitotic cell lysates treated with RO3306 or DMSO as a control. There was no difference in Sas-6 levels between the two groups (Fig. S5*A*). Cells expressing GFP-Sas-6 WT, 2A, or 2D were subsequently treated with or without the proteasome inhibitor MG132, and the protein expression level, ubiquitination modification, and half-life were measured. Phosphorylation of Sas-6 did not affect its degradation (Fig. S5, *B*–*D*). These results indicate that CDK1-cyclin B–mediated Sas-6 disassociation from the centriole during early mitosis and APC/C^{Cdh1}-mediated Sas-6 degradation from late mitosis to G1 phase are two independent events, both of which jointly lead to the removal of Sas-6 from the centriole; hence, a decrease in centriolar GFP-Sas-6 was observed after entry into mitosis (Fig. S1, *B*, *C* and Movie S1). Furthermore, most of the centriolar Sas-6 was removed before anaphase, indicating a leading role for cyclin B-mediated Sas-6 dissociation in this process (Figs. S1, *B*, *C*, 3, *A* and *B*).

The centriole engagement configuration was affected by the presence or absence of Sas-6 or the cartwheel; therefore, we examined the engagement configuration within one pair of centrioles in GFP-Sas-6 WT, 2A, 2D, or 2E-expressing cells during mitotic exit or early G1 phase. The vast majority of GFP-Sas-6 WT-, 2D-, and 2E-expressing cells (∼90%, ∼92%, ∼92%) displaying disassembled cartwheels or no detectable centriolar GFP signal underwent mother/daughter centriole disengagement, whereas roughly ∼23% of GFP-2A-expressing cells steadily retained centriolar GFP-2A and maintained engagement of paired mother/daughter centrioles (Fig. S6, *A* and *B*), suggesting that the removal of Sas-6 regulated by CDK-cyclin B further positively regulated centriole disengagement.

We subsequently analyzed the effect of abnormal centriole engagement caused by unphosphorylated Sas-6 and the

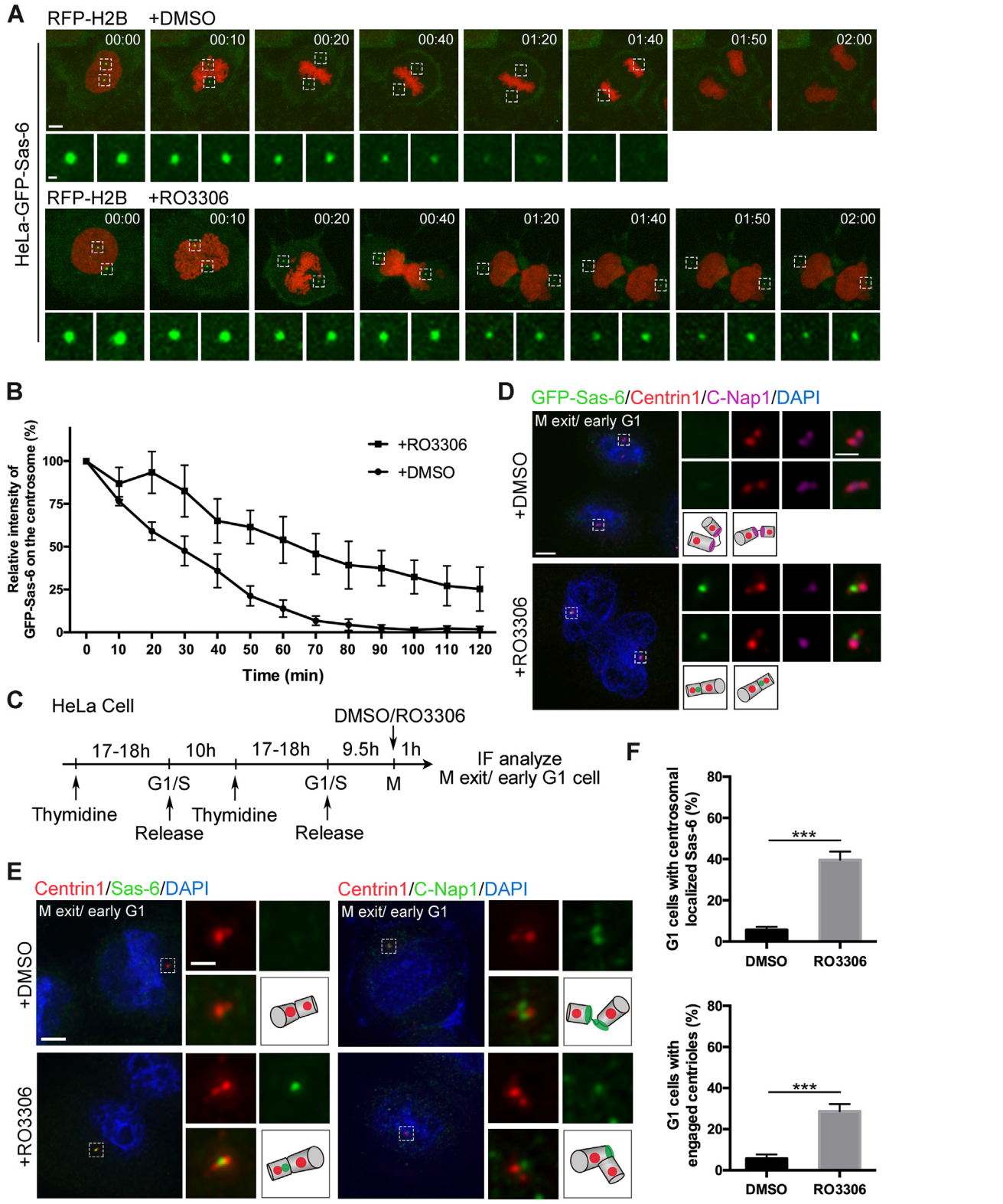

Figure 3. CDK1-cyclin B triggers Sas-6 removal and centriole disengagement during mitotic exit. *A*, inhibition of CDK1-cyclin B activity prevents Sas-6 removal from centrioles during mitotic exit. HeLa cells stably expressing GFP-Sas-6 were transfected with RFP-H2B, treated with DMSO or 9 μM RO3306, and filmed for 2 h from nuclear envelope breakdown (NEBD) to mitotic exit. Images were captured every 5 min, and 30 slices at an 18-μm Z-section thickness were obtained. Scale bar, 5 μm (large images) or 1 μm (inset images) (see also Movies S2 and S3). *B*, line graphs showing the mean centriolar GFP-Sas-6 fluorescence intensity in the experiments described in (*A*). Measurements were obtained for 10 centrosomes in three independent experiments. Error bars represent the mean ± SD. *C*, experimental scheme for generating mitotic exit/early G1 phase HeLa cells by CDK1-cyclin B inhibition. HeLa cells were arrested at G1/S transition by thymidine treatment, released for 9.5 h, and treated with DMSO or RO3306 for 1 h to mitotic exit/early G1 phase. *D and E*, inhibition of CDK1-cyclin B activity prevents Sas-6 removal and centriole disengagement at early G1 phase. HeLa cells stably expressing GFP-Sas-6 (D) or HeLa cells (E) treated using the method described in (*C*) were fixed with methanol and analyzed by immunofluorescence using the indicated antibodies. DNA was stained

persistent presence of the cartwheel on procentriole formation in postmitotic cells. Since disengagement of mother/daughter centrioles is a prerequisite for the initiation of a new centrosome cycle (6, 7), and CDK1-cyclin B phosphorylation promotes centriolar Sas-6 disassociation and paired centriole disengagement during mitosis, we conducted an immunofluorescence assay to evaluate whether the persistent localization of unphosphorylatable 2A on centrioles inhibits procentriole formation in the subsequent centrosome cycle. Sas-6 WT overexpression promoted the formation of excess procentrioles or centrioles as previously reported (14), while overexpression of GFP-Sas-6 2A induced significantly less centriole production than WT and 2D in both asynchronized and S phase-synchronized cells (Figs. 4, *D*, *E*, S6, *C*, and *D*), indicating that the persistent localization of Sas-6-2A on centrioles prevented centriole disengagement, which further inhibited centriole reduplication.

Collectively, these results demonstrate that centriolar Sas-6 removal mediated by CDK1-cyclin B promotes its disassociation and translocation to the cytoplasm. APC/C^{Cdh1} subsequently targets and ubiquitinates Sas-6 for degradation, leading to disengagement of the paired centrioles and licensing of a new round of centriole duplication.

Phosphorylation of Sas-6 by CDK1-cyclin B disrupts the STIL–Sas-6 complex

To investigate the manner by which CDK1-cyclin B–mediated phosphorylation triggers centriolar Sas-6 disassociation, we first examined the centriolar localization of Sas-6 and its interaction with STIL, another cartwheel component and centriole duplication initiator, which facilitates the loading of Sas-6 onto centrioles during early S phase (25–29, 38–40). Immunofluorescence microscopy demonstrates that centriolar STIL disappeared immediately before Sas-6 at metaphase (Fig. 5*A*). Moreover, immunoprecipitation shows that while Sas-6 was bound to STIL during interphase, their interaction was significantly diminished as cells entered mitosis (Fig. 5*B*).

Since CDK1-cyclin B activity is also required for the translocation of STIL from the centriole to the cytoplasm (48), we evaluated whether CDK1-cyclin B–mediated phosphorylation of Sas-6 disrupts the interaction between Sas-6 and STIL, thus triggering their release from the centriole and leading to disassembly of the cartwheel. Following treatment of cells with RO3306, both centriolar Sas-6 and STIL remained stable throughout mitosis and the binding of Sas-6 to STIL increased (Fig. 5, *C* and *D*), indicating that CDK1 activity was required for disassociation of the Sas-6–STIL complex and removal of both components from the centriole. For confirmation, we further analyzed the centriolar localization of STIL in metaphase HeLa cells expressing GFP-Sas-6 WT, 2A, or 2D. Quantitation of STIL immunofluorescence on the centrioles demonstrates that 2A efficiently stabilized centriolar STIL at metaphase (Fig. 5, *E* and *F*). Consistently, immunoprecipitation shows that the interaction between STIL and 2A was much stronger than that between STIL and WT or 2D (Figs. 5, *G*, *H* and S7, *A*–*C*). By contrast, phosphorylation of Sas-6 by CDK1-cyclin B did not affect its self-polymerization or interaction with the other cartwheel components CEP135 and CPAP (Fig. S7, *D*–*F*). Taken together, these results demonstrate that Sas-6 phosphorylation by CDK1-cyclin B disrupts its binding to STIL, leading to their release from the cartwheel and cartwheel disassembly.

Phosphorylation of Sas-6 by CDK1-cyclin B weakens the binding between Sas-6 and Nedd1

Since our previous research demonstrates that Plk4 phosphorylates the PCM component Nedd1, regulates its binding to Sas-6, and recruits Sas-6 onto the mother centriole to initiate cartwheel assembly in cooperation with STIL (24), we examined whether Nedd1 participates in the regulation of centriolar Sas-6 removal triggered by CDK1-cyclin B during mitosis. Nedd1 immunofluorescence localized to centrosomes throughout the cell cycle and partially colocalized with Sas-6 at centrioles (Fig. 6*A*). Immunoprecipitation reveals that GFP-Sas-6 strongly bound to Nedd1 and γ-tubulin, the main component of γ-TuRC essential for daughter centriole biogenesis (Fig. 6*B*). Following treatment of cells with RO3306, the binding of Sas-6 to Nedd1 and γ-tubulin increased (Fig. 6*C*). In mitotic cells expressing GFP-Sas-6 WT, 2A, or 2D, Nedd1 and γ-tubulin were bound to unphosphorylatable 2A more strongly than to Sas-6 WT or the phosphorylated-mimic 2D (Fig. 6*D*). Furthermore, GFP-Nedd1 specifically interacted with endogenous Sas-6 but not STIL (Fig. 6*E*). Knockdown of Nedd1 perturbed the continuous loading of Sas-6 and STIL onto centrioles from S phase to early mitosis, whereas depletion of Sas-6 and STIL had no effect on the centrosomal localization of Nedd1 (Fig. 6, *F* and *G*). These results indicate that Nedd1 acts upstream of Sas-6 and STIL, Sas-6 serves as a connective factor between Nedd1 and STIL, and Sas-6 and STIL mutually affect the localization of each other during the maintenance of cartwheel structure.

Collectively, we conclude that the phosphorylation of Sas-6 by CDK1-cyclin B disrupts its interactions with STIL and Nedd1 and that Nedd1 is persistently located on centrioles during the cell cycle, both of which eventually cause the sequential release of STIL and Sas-6 from the cartwheel, facilitating centriole disengagement and licensing centriole duplication in the next cell cycle (Fig. 6*H*).

Discussion

We demonstrate that immobilization of Sas-6 to the basal lumen of the daughter centriole after the initiation of centriole biogenesis (30) maintains association of the daughter and mother centrioles and prevents their premature

with DAPI. Scale bars, 5 μm (large images) or 1 μm (inset images). *F*, quantitation of mitotic exit/G1 cells according to Sas-6 staining and engaged centrioles in (*E*). Approximately 200 cells were counted per sample, and three independent experiments were conducted. The statistical data are expressed as the mean ± SD. ***$p < 0.001$ (Student's *t* test).

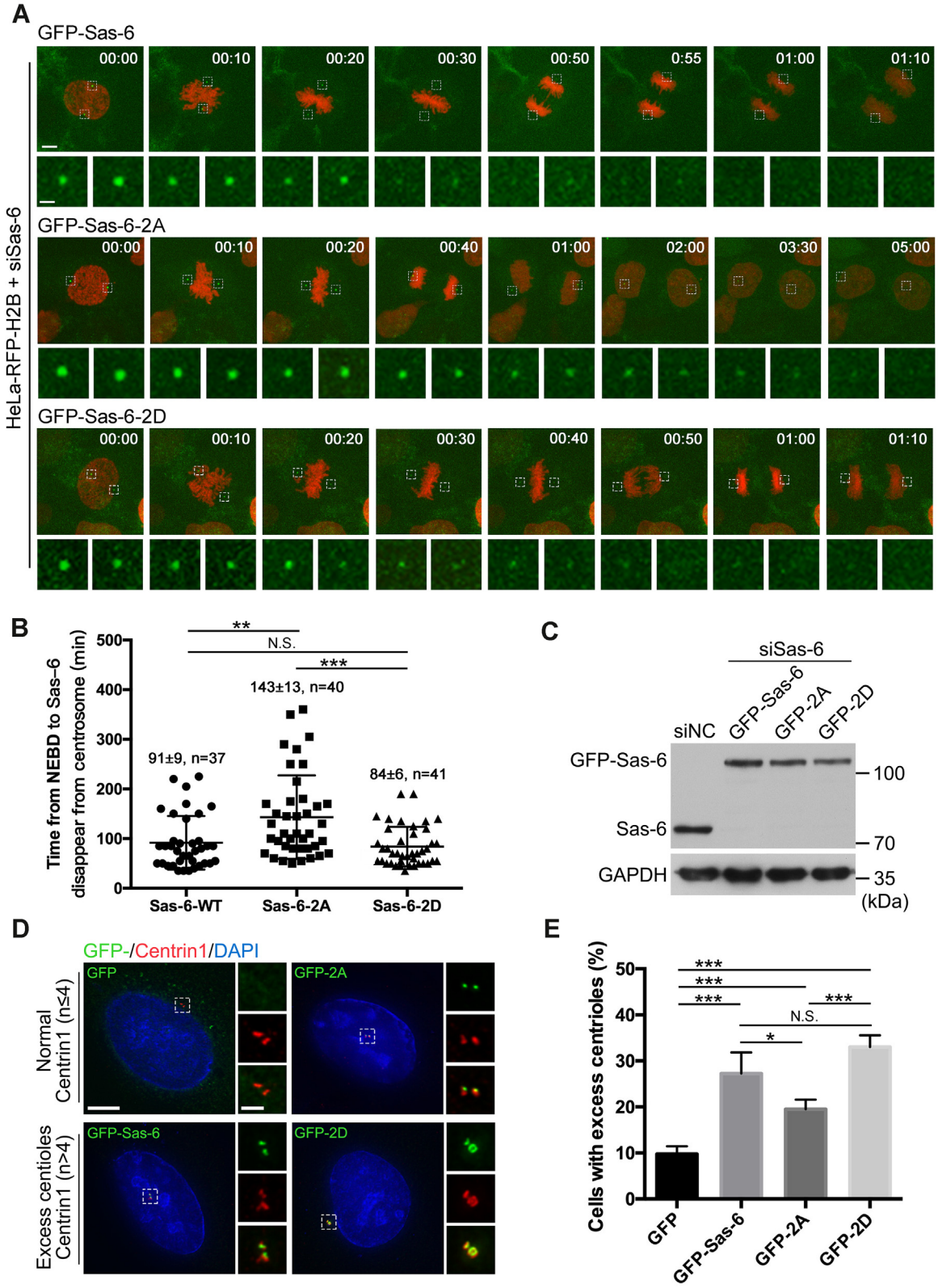

Figure 4. Phosphorylation of Sas-6 by CDK1-cyclin B promotes the disassociation of Sas-6 from mitotic centrioles and licenses centriole reduplication. *A*, Sas-6 2A is released from the centriole at a slower rate than WT and Sas-6 2D. HeLa cells stably expressing RFP-H2B were cotransfected with siSas-6 and GFP-Sas-6, 2A, or 2D and filmed for 6 h from nuclear envelope breakdown (NEBD) to G1 phase. Images were captured every 5 min, and 30 slices at an 18-μm Z-section thickness were obtained. Scale bar, 5 μm (large images) or 1 μm (inset images) (see also Movies S4–S6). *B*, quantitation of the time from NEBD to the disappearance of GFP-Sas-6, 2A, or 2D from the centriole shown in (*A*). The timing of Sas-6 disappearance from centrioles is judged as the same Sas-6 intensity between centrioles and the cytoplasm. Error bars indicate the mean ± SEM from three independent experiments. Not significant (N.S.), $^{**}p < 0.01$, $^{***}p < 0.001$ (unpaired *t* test). *C*, Sas-6 siRNA knockdown-and-rescue efficiency. HeLa cells were treated as described in (*A*), harvested, and analyzed by immunoblotting using antibodies against Sas-6 and GAPDH. *D*, GFP-tagged 2A exhibits a slightly weaker ability to cause centriole reduplication.

disengagement and disintegration of the centrosomes during S phase to late G2 phase. Phosphorylation of Sas-6 by CDK1-cyclin B promotes its release from the cartwheel in early mitosis and permits disengagement of the daughter centriole from its mother during mitotic exit. These findings facilitate a better understanding of the key questions related to why the cartwheel persists after daughter centriole biogenesis until the procentriole matures, how engagement and disengagement of the paired mother and daughter centrioles are regulated for accurate centrosome cycling, and how the centrosome cycle is regulated by the cell cycle machinery.

The orthogonal engagement configuration between the daughter and mother centrioles after daughter centriole biogenesis appears to restrain reduplication for centriole number stability until their disengagement from mitotic exit to the next early G1 phase and subsequent initiation of a new round of duplication (6, 7). Thus, the engagement configuration acts as an "on-and-off switch" for the initiation of centriole duplication, and this process is mainly regulated by protease separase and Plk1 (7, 49–52). Engagement of the paired centrioles has been proposed to be held by the cohesin ring complex and surrounding PCM (41–43, 53). Separase-dependent cleavage of the cohesin ring subunit Scc1 and PCM component PCNT results in centriole disengagement (44, 45, 50, 53). In comparison, Plk1 likely regulates the disengagement process by phosphorylating PCNT and enhancing its cleavage by separase. Plk1 also regulates the degradation of Cep68 and cleavage of PCNT to allow Cep215 removal from the PCM, ensuring the fidelity of centriole disengagement, separation, and licensing (42, 46). In addition, recent studies indicate that mother centriole-localized Cep57 and Cep57L1 cooperatively maintain centriolar engagement during interphase (54, 55). However, it remains elusive whether there exists a direct linker localized on the daughter centriole that holds the paired centrioles together during the S phase and G2 phase, which is then dismissed in a regulated manner for disengagement of the centriole pair during mitosis. Here, we demonstrate that Sas-6 serves as a linker to maintain engagement of the daughter and mother centrioles after daughter centriole biogenesis. Sas-6 connects upstream to Nedd1 on the mother centriole and downstream to STIL and γ-TuRC on the daughter centriole. This Sas-6 linker is strengthened by its continuous accumulation and persistence until its phosphorylation by CDK1-cyclin B during mitotic entry. This phosphorylation of Sas-6 disrupts its association with Nedd1, STIL, and γ-TuRC, leading to cartwheel disassembly, paired centriole disengagement, and licensing of a new round of centriole biogenesis in the subsequent G1/S transition.

However, unlike in human cells, the cartwheel/Sas-6 is a permanent scaffolding structure in *Drosophila*, in which the centriole pairs can become disengaged without cartwheel disassembly (3). It is possible that CDK1-cyclin B negatively regulates the association of mother centriole-localized factors with Sas-6 but does not directly regulate Sas-6, causing the cartwheel to lose connection with the mother centriole without cartwheel disassembly. This is supported by the multiple sequence alignment in Fig. 2*D*, which shows that human Sas-6 phosphorylation sites mediated by CDK1-cyclin B, as well as the nearby C-terminal sequence, are missing from homologous Sas-6 in *Drosophila*. If this is the case, the cartwheel/Sas-6 would provide an additional layer of regulation to maintain centriole engagement, in addition to the PCM and cohesin ring complex pathway, to enable disengagement of centriole pairs in *Drosophila* without cartwheel disassembly. Periodic assembly/disassembly of the cartwheel renders centriole engagement/disengagement regulation and the centrosome cycle more faithful and accurate.

Based on our present and previously reported data, we propose a working model to illustrate the functions of Sas-6 in centriole engagement and disengagement under the regulation of CDK1-cyclin B and other cell cycle regulators in human cells (Fig. 7). During G1/S transition, Plk4 binds to and phosphorylates STIL and Nedd1 to allow loading of Sas-6 onto the mother centriole for cartwheel assembly and daughter centriole biogenesis (24–29). As cells enter the S phase and G2 phase, Sas-6 is progressively recruited and immobilized onto the centrioles to maintain association of the paired mother and daughter centrioles and the integrity of the centrosome (30, 37). As cells enter mitosis, CDK1-cyclin B phosphorylates STIL, Nedd1 (48, 56, 57), and Sas-6 and weakens the association between Sas-6, STIL, and Nedd1 to trigger the release of Sas-6 and STIL from the centrioles, facilitating disassembly of the cartwheel and disengagement of the daughter and mother centrioles (Fig. 7*A*). By contrast, blocking CDK1-cyclin B-mediated phosphorylation of Sas-6 inhibits its disassociation from centrosomal STIL and Nedd1, restraining cartwheel disassembly and leading to the failure of paired centriole disengagement and delay of a new round of centriole duplication (Fig. 7*B*). In summary, we uncover that Sas-6 stabilizes centriole engagement after daughter centriole biogenesis by linking the cartwheel and daughter centriole with the mother centriole. Sas-6 is eventually released from the cartwheel to allow disengagement of the daughter and mother centrioles during mitosis under the regulation of CDK1-cyclin B for the licensing of a new round of centrosome duplication, although we do not exclude other mitotic kinases may also contribute to phosphorylation and this function of Sas-6.

Experimental procedures

Cell culture, transfection, synchronization, and drug treatment

HEK293, HeLa, and U2OS cells were obtained from American Type Culture Collection and cultured in Dulbecco's Modified Eagle's Medium (Gibco) supplemented with 10% fetal bovine serum at 37 °C in a 5% CO_2 atmosphere.

HeLa cells were cotransfected with siSas-6 and GFP-tagged Sas-6 WT, 2A, or 2D for 72 h, fixed with methanol, and analyzed by immunofluorescence using an antibody against Centrin1. DNA was stained with DAPI. Scale bars, 5 μm (large images) or 1 μm (inset images). *E*, quantitation of transfected cells possessing excess centrioles in (D). Approximately 200 cells were counted per sample, and four independent experiments were conducted. The statistical data are expressed as the mean ± SD. Not significant (N.S.), $*p < 0.05$, $***p < 0.001$ (Student's *t* test). See also Figs. S5 and S6.

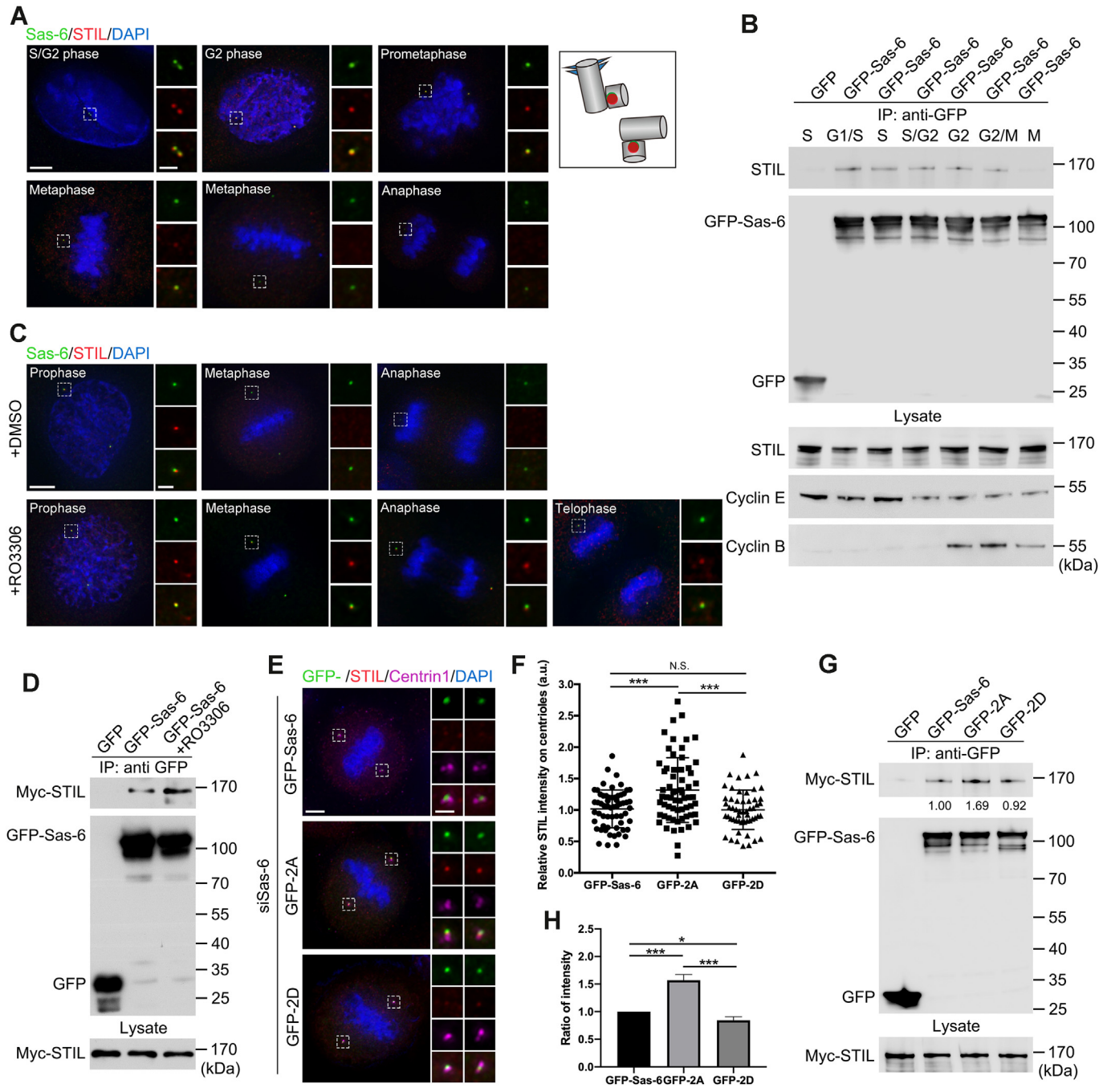

Figure 5. Phosphorylation of Sas-6 by CDK1-Cyclin B disrupts the STIL–Sas-6 complex. *A*, Sas-6 colocalizes with STIL at the daughter centrioles from S phase to prophase. HeLa cells were fixed with methanol and analyzed by immunofluorescence using antibodies against Sas-6 and STIL. *B*, Sas-6 interacts with STIL from G1/S phase to G2/M phase. HEK293 cells transfected with GFP or GFP-tagged Sas-6 were arrested at G1/S transition by thymidine treatment and subsequently released, harvested at the indicated time points for immunoprecipitation using GFP-trap beads, and analyzed by immunoblotting using the indicated antibodies. *C*, inhibition of CDK1-cyclin B activity prevents centriolar Sas-6 and STIL from disappearing during late mitosis. HeLa cells were arrested at G1/S transition by thymidine treatment, released for 9.5 h to mitosis, and treated with DMSO or RO3306 for 15 min. Cells were fixed with methanol and analyzed by immunofluorescence using antibodies against Sas-6 and STIL. *D*, inhibition of CDK1-Cyclin B activity enhances the interaction between Sas-6 and STIL during mitosis. HEK293 cells cotransfected with Myc-STIL and GFP or GFP-tagged Sas-6 were arrested at mitosis by thymidine-nocodazole treatment and subsequently treated with DMSO or RO3306 for 15 min. Cells were harvested for immunoprecipitation with GFP antibody-conjugated beads and analyzed by immunoblotting using antibodies against Myc and GFP. *E*, Sas-6 mutant 2A inhibits the disappearance of centriolar STIL at metaphase. HeLa cells cotransfected with siSas-6 and GFP-Sas-6 WT, 2A, or 2D were arrested at G1/S transition by thymidine treatment and released for 10 h to mitosis. Cells were fixed with methanol and analyzed by immunofluorescence using antibodies against STIL and Centrin1. *F*, quantitation of the relative STIL immunofluorescence on the metaphase centrioles in (*E*). Approximately 60 cells in three independent experiments were analyzed. The average cytoplasmic immunofluorescence intensity was subtracted as background. The statistical data are expressed as the mean ± SD. Not significant (N.S.), ***$p < 0.001$ (Student's *t* test). *G*, Sas-6 phosphorylation weakens the interaction between Sas-6 and STIL. HEK293 cells cotransfected with Myc-STIL and GFP, GFP-Sas-6 WT, 2A, or 2D were arrested at mitosis by thymidine-nocodazole treatment, harvested for immunoprecipitation with GFP antibody-conjugated beads, and analyzed by immunoblotting using the indicated antibodies. Three independent experiments were performed (Figs. 5*G*, S7, *A* and *B*). *H*, quantitation of the interaction between Myc-STIL and GFP-tagged Sas-6 WT, 2A, or 2D in (Figs. 5*G*, S7, *A* and *B*). The protein–protein interaction discrepancy was quantitated using ImageJ. The relative interaction between Sas-6 and STIL was normalized to immunoprecipitated Sas-6 by ImageJ quantitation. The value of the Sas-6 group was set as 1.0, relative to which the other mutant groups were calculated. DNA was stained with DAPI. Scale bars, 5 μm (large images) or 1 μm (inset images). See also Fig. S7.

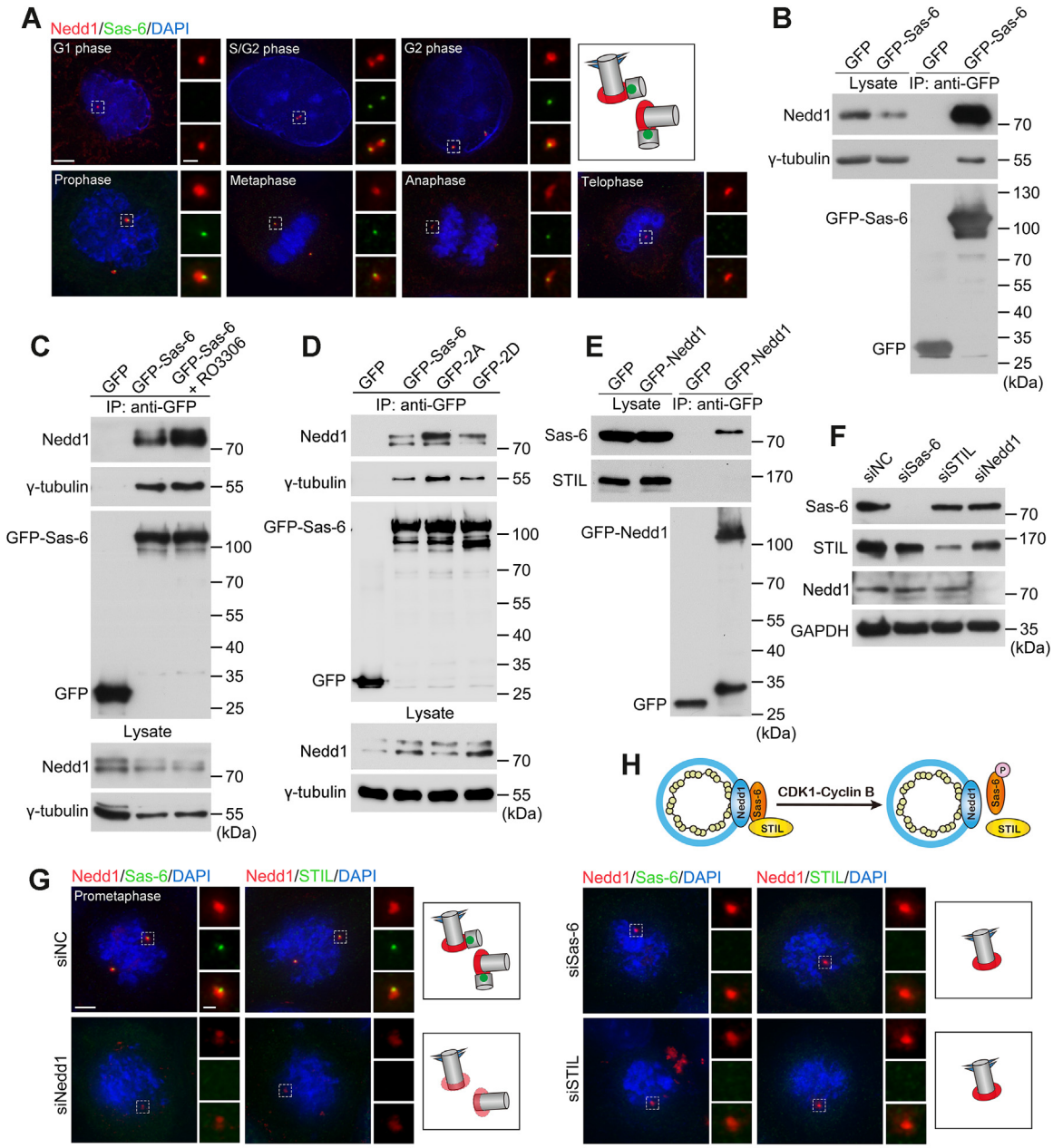

Figure 6. Phosphorylation of Sas-6 weakens the interaction between Sas-6 and Nedd1. *A*, Sas-6 partially colocalizes with Nedd1 at the centrosomes. HeLa cells were fixed with methanol and analyzed by immunofluorescence using antibodies against Sas-6 and Nedd1. *B*, Sas-6 interacts with Nedd1 and γ-tubulin in cells. HEK293 cells transfected with GFP or GFP-tagged Sas-6 were harvested for immunoprecipitation with GFP-Trap beads and analyzed by immunoblotting using antibodies against Nedd1, γ-tubulin, and GFP. *C*, inhibition of CDK1-cyclin B kinase activity strengthens the binding of Sas-6 with Nedd1 and γ-tubulin during mitosis. HEK293 cells transfected with GFP or GFP-Sas-6 were arrested in mitosis by thymidine-nocodazole treatment, and DMSO or RO3306 was added for 15 min prior to harvest. Cell lysates were immunoprecipitated with GFP-Trap beads and analyzed by immunoblotting using antibodies against Nedd1, γ-tubulin, and GFP. *D*, Sas-6 phosphorylation by CDK1-cyclin B weakens the interaction between Sas-6 and Nedd1. HEK293 cells transfected with GFP, GFP-Sas-6 WT, 2A, or 2D were arrested in mitosis by thymidine-nocodazole treatment, harvested for immunoprecipitation with GFP-Trap beads, and analyzed by immunoblotting using antibodies against Nedd1, γ-tubulin, and GFP. Three independent experiments were performed, but only one representative result is shown in (*C* and *D*). *E*, Nedd1 specifically interacts with Sas-6 but not STIL. HEK293 cells transfected with GFP or GFP-tagged Nedd1 were harvested for immunoprecipitation with GFP-Trap beads and analyzed by immunoblotting using antibodies against Sas-6, STIL, and GFP. *F*, Sas-6, STIL, and Nedd1 siRNA knockdown efficiency. HeLa cells were transfected with the indicated siRNA for 72 h and subsequently harvested and analyzed by immunoblotting using the indicated antibodies. *G*, Nedd1 acts upstream of Sas-6 and STIL. HeLa cells were treated with siRNA against Sas-6, STIL, and Nedd1 and analyzed by immunofluorescence using the indicated antibodies. Note that Nedd1 knockdown abolishes centriolar Sas-6 and STIL in prometaphase cells, whereas Sas-6 or STIL knockdown has no effect on the centrosomal localization of Nedd1. *H*, schematic diagram illustrating the relationship among Nedd1, Sas-6, and STIL regulated by CDK1-cyclin B. DNA was stained with DAPI. Scale bars, 5 μm (large images) or 1 μm (inset images).

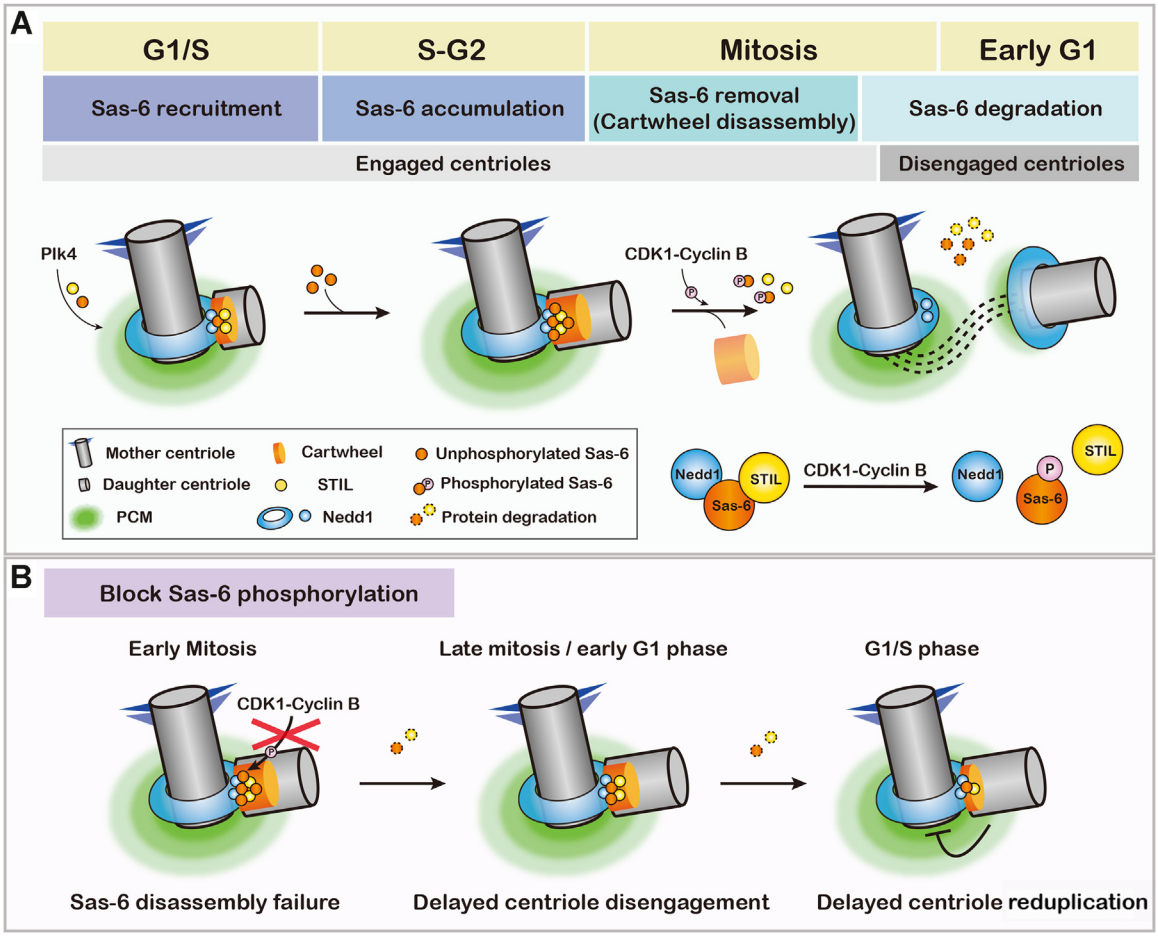

Figure 7. A proposed working model indicating that the Sas-6-assembled cartwheel structure is involved in centriole engagement and disengagement under CDK1-cyclin B control. *A*, during G1/S transition, Plk4 binds and phosphorylates STIL and Nedd1 to recruit Sas-6 onto the lateral proximal end of the mother centriole in order to initiate cartwheel assembly and daughter centriole biogenesis. As cells progress through S phase and G2 phase, Sas-6 is progressively recruited and immobilized at the base of the daughter centriole lumen to maintain engagement of the paired daughter and mother centrioles and integrity of the centrosomes. During mitosis, CDK1-cyclin B phosphorylates Sas-6 at T495 and S510, which weakens the association of Sas-6 with STIL and Nedd1 and triggers the translocation of STIL and Sas-6 from the daughter centriole to the cytoplasm, thus facilitating cartwheel disassembly and daughter centriole disengagement from the mother centriole. *B*, conversely, blocking CDK1-cyclin B–mediated phosphorylation of Sas-6 inhibits its disassociation from STIL and Nedd1, thus restraining disassembly of the cartwheel and delaying centriole disengagement and a new round of centriole duplication. Plk4, Polo-like kinase 4.

For plasmid or siRNA transfection of cells, Lipofectamine 2000 (Invitrogen) was used according to the manufacturer's instructions.

Cells were synchronized at G1/S transition using the double-thymidine blockade method. Briefly, cells were treated with 2.5 mM thymidine (Sigma) for 17 to 21 h, released for 10 h, and treated again with 2.5 mM thymidine for a further 17 to 21 h to obtain G1/S phase-arrested cells. Subsequently, cells were released into fresh medium for 0 to 6 h to S phase, 6 to 10 h to G2 phase, or 10 to 12 h to mitosis.

Alternatively, cells were first synchronized at prometaphase by thymidine-nocodazole treatment. Briefly, cells were treated with 2.5 mM thymidine for 17 to 21 h, released, and treated with 100 ng/ml nocodazole for 14 to 16 h to obtain prometaphase-arrested cells. Subsequently, cells were released and harvested at the indicated time points.

For drug treatment, the compounds, concentrations, and treatment times used in this study are as follows: 0.1 μM BI2536 for 2 h, 9 μM RO3306 for 15 min, 0.25 μM MLN8237 for 30 min, 0.2 μM AZD1152 for 30 min, 1 μM ZM447439 for 30 min, and DMSO as a negative control. Mitotic cells were treated with the indicated drug before harvest. All drug were used and verified according the manufacturer's instructions, and all drug concentrations and incubation times were tightly controlled to avoid inducing mitotic exit (Figs. 2*B* and S4*C*).

Stable GFP-Sas-6–expressing HeLa cell lines were generated by lentivirus infection. Briefly, pCDH-CMV-MCS-EF1-Puro-GFP-Sas-6 was introduced into HEK293T cells together with psPAX2 and pMD2G. This recombinant lentivirus was then used to infect HeLa cells, and the population expressing GFP-Sas-6 was selected using puromycin. To generate stable RFP-H2B-expressing HeLa cell lines, HeLa cells were transfected with RFP-H2B, and stable clones were selected using G418.

Plasmids, siRNA, and antibodies

Human Sas-6 was cloned from the cDNA library and inserted into the pEGFP-C1 or pCMV-Myc vector. The Sas-6 point mutations S111A, T495A, S510A, S657A, 2A (T495A

and S510A), 2D (T495D and S510D), and 2E (T495E and S510E) were generated by PCR using site-directed mutagenesis primers. GFP-Sas-6 was subcloned from pEGFP-C1-Sas-6 into the pCDH-CMV-MCS-EF1-Puro lentivirus vector. The Myc-GFP-STIL plasmid was a gift from Dr Andrew J. Holland (Johns Hopkins University School of Medicine), and pEGFP-C1-Cep135 was kindly provided by Dr Tang K. Tang (Institute of Biomedical Sciences, Academia Sinica). STIL and Cep135 were amplified from these plasmids by PCR and inserted into the pCMV-Myc vector. Human Nedd1 was cloned from the cDNA library and inserted into the pEGFP-C1 vector. Sas-6 siRNA (3′UTR, 5′-GAGCUGUUAAAGACUGGAUAC UUUA-3′), STIL siRNA (5′-GUUUAAGGGAAAAGUUA UUTT-3′), CPAP siRNA (5′-AGAAUUAGCUCGAAUAG AAUU-3′), Nedd1 siRNA (5′-GGGCAAAAGCAGACAUGU GTT-3′), and a non-targeting negative control siRNA were synthesized by GenePharma.

The anti-GFP antibody used for immunoprecipitation was generated by the immunization of rabbits with bacterially expressed recombinant His-tagged GFP. The phospho-S510-Sas-6 antibody was generated by the immunization of rabbits with a phosphorylated peptide (506-RSGI(S-p)PNLN-514) (Abclonal). Other antibodies used in this study include mouse anti-Sas-6 (Santa Cruz Biotechnology, sc-81431), rabbit anti-Centrin1 (Proteintech, 12794-1-AP), mouse anti-Centrin1 (Merck Millipore, 20H5), rabbit anti-STIL (Abcam, ab89314), mouse anti-Nedd1 (residues 341-end) (56), rabbit anti-Nedd1 (Sigma, HPA038591), rabbit anti-CPAP (Proteintech, 11517-1-AP), rabbit anti-PCNT (Abcam, ab4448), rabbit anti-CDK5RAP2 (Abcam, ab70213), rabbit anti-γ-tubulin (Sigma, T3559), mouse anti-Cyclin E (Santa Cruz Biotechnology, sc-247), mouse anti-Cyclin B (Santa Cruz Biotechnology, sc-25764), rabbit anti-H3pS10 (Thermo Fisher Scientific, 44–1190G), mouse anti-GFP (Proteintech, 66002-1-Ig), mouse anti-Myc (Sigma, M4439), mouse anti-GAPDH (Proteintech, 60004-1-Ig), mouse anti-α-tubulin (Sigma, T9026), mouse anti-C-Nap1 (Santa Cruz Biotechnology, sc-390540), rabbit anti-Plk1 (pT210) (Cell Signaling Technology, #9062), and rabbit anti-Aurora A (pT288)/Aurora B (pT232)/Aurora C (pT198) (Cell Signaling Technology, #2914). Dilutions of the commercial antibodies were performed according to the manufacturer's protocol.

All animal experiments were performed in the Laboratory Animal Center of Peking University following the National Institutes of Health Guide for the Care and Use of Laboratory Animals guidelines approved by the Institutional Animal Care and Use Committee at Peking University.

Immunoprecipitation

Cells transfected with the indicated constructs were washed with cold PBS and lysed in immunoprecipitation buffer (20 mM Tris-HCl, pH 8.0, 150 mM NaCl, 0.5% NP-40, 5 mM NaF, 2 mM EGTA, 0.5 mM EDTA, 1 mM Na_3VO_4, 1 mM PMSF, and protease inhibitors) at 4 °C for 15 min. Subsequently, the lysates were centrifuged at 15,000*g* for 15 min, and the supernatants were collected and incubated with GFP antibody-conjugated beads or GFP-Trap beads (Chromo Tek, gtc-20) at 4 °C for 2 h. After extensive washing with immunoprecipitation buffer, the beads were resuspended in sample buffer and boiled at 95 °C for 10 min. Proteins eluted from the beads were analyzed by SDS-PAGE and immunoblotting.

Phos-tag assay, in vitro kinase assay, and MS

Phos-tag is a novel phosphate-binding tag at neutral pH that is used for the separation, purification, and detection of phosphorylated proteins. Protein samples were analyzed by 8% SDS-PAGE containing 25 μM Phos-tag (Wako) and 50 μM MnCl2 in a resolving gel. After electrophoresis, the gel was soaked in a general transfer buffer containing 1 mM EDTA for 10 min with gentle agitation and then in transfer buffer without EDTA for a further 10 min before being transferred onto PVDF membrane using a wet-tank method. Phosphorylated proteins were analyzed by immunoblotting.

For the *in vitro* kinase assay, ∼2 μg GFP-tagged Sas-6, 2A, or Nedd1 protein expressed in and purified from HEK293 cells was incubated at 30 °C for 30 min with 50 ng recombinant human CDK1-cyclin B (New England Biolabs) in NEBuffer supplemented with 200 mM ATP and 10 μCi γ-^{32}P ATP. The reaction was quenched with sample buffer and analyzed by SDS-PAGE and autoradiography.

For MS, HEK293 cells transfected with GFP-Sas-6 were arrested at G1/S phase or prometaphase, and whole-cell lysates were immunoprecipitated using GFP-Trap beads and analyzed by SDS-PAGE. GFP-Sas-6 was visualized by Coomassie Brilliant Blue and processed for MS analysis to identify Sas-6 modification.

Immunofluorescence, live-cell imaging, and statistical analysis

For immunofluorescence, cells grown on coverslips were fixed in −20 °C precooled methanol for 5 min and incubated with the indicated primary antibodies overnight at 4 °C. After washing three times in PBS, the coverslips were incubated with the indicated secondary antibodies at room temperature for 1 h, mounted with Mowiol containing 1 μg/ml DAPI, and observed under a Delta Vision Elite microscope. Images were captured at a 1.2-μm Z-section thickness in six slices for interphase cells or a 4-μm Z-section thickness in 20 slices for mitotic cells and processed for maximum intensity projection. The fluorescence intensity and spindle length were measured using the Volocity software.

For live-cell imaging, cells were plated on glass-bottomed dishes and transfected with the indicated plasmids. Subsequently, cells were viewed under a high-speed spinning-disk confocal microscope, and the data were processed using the Fusion software. Images were captured at an 18-μm Z-section thickness in 30 slices every 5 or 10 min. Fluorescence intensity of the GFP-tagged Sas-6 proteins was measured using the Volocity software. All statistical analyses were performed using the GraphPad Prism 6 software.

Data availability

All pertinent data are provided in the main text and supporting information. All of the reagents included in this study are available on request from the corresponding author.

Supporting information—This article contains supporting information.

Acknowledgments—We are very appreciative to Drs. Andrew J. Holland (Johns Hopkins University School of Medicine) and Tang K. Tang (Institute of Biomedical Sciences, Academia Sinica) for generously supplying reagents. We thank the Core Facilities at the National Center for Protein Sciences at Peking University and the College of Life Sciences of Peking University, particularly Drs. Hongxia Lv, Dong Liu, Siying Qin, and Chunyan Shan, for assistance with imaging, MS analysis, and data analysis. We thank all the members of our laboratory for their constructive suggestions.

Author contributions—C. M. Z. conceptualization; F. H., X. W. X., G. W. X., and B. Y. Z. methodology; F. H., X. W. X., G. W. X., and B. Y. Z. investigation; C. M. Z., F. H., and Q. J. formal analysis; C. M. Z., F. H., and Q. J. writing-original draft.

Funding and additional information—This work was supported by grants from the National Natural Science Foundation of China (NSFC) (32130026, 91854204 and 32070714).

Conflict of interest—The authors declare that they have no conflicts of interest regarding the content of this article.

Abbreviations—The abbreviations used are: PCM, pericentriolar matrix; Plk4, Polo-like kinase 4.

References

1. Bettencourt-Dias, M., and Glover, D. M. (2007) Centrosome biogenesis and function: centrosomics brings new understanding. *Nat. Rev. Mol. Cell Biol.* **8**, 451–463
2. Nigg, E. A., and Raff, J. W. (2009) Centrioles, centrosomes, and cilia in health and disease. *Cell* **139**, 663–678
3. Nigg, E. A., and Holland, A. J. (2018) Once and only once: mechanisms of centriole duplication and their deregulation in disease. *Nat. Rev. Mol. Cell Biol.* **19**, 297–312
4. Fu, J., and Zhang, C. (2019) Super-resolution microscopy: successful applications in centrosome study and beyond. *Biophys. Rep.* **5**, 235–243
5. Wang, G., Jiang, Q., and Zhang, C. (2014) The role of mitotic kinases in coupling the centrosome cycle with the assembly of the mitotic spindle. *J. Cell Sci.* **127**, 4111–4122
6. Tsou, M. F., and Stearns, T. (2006) Controlling centrosome number: licenses and blocks. *Curr. Opin. Cell Biol.* **18**, 74–78
7. Tsou, M. F., and Stearns, T. (2006) Mechanism limiting centrosome duplication to once per cell cycle. *Nature* **442**, 947–951
8. Carvalho-Santos, Z., Machado, P., Branco, P., Tavares-Cadete, F., Rodrigues-Martins, A., Pereira-Leal, J. B., *et al.* (2010) Stepwise evolution of the centriole-assembly pathway. *J. Cell Sci.* **123**, 1414–1426
9. Conduit, P. T., Wainman, A., and Raff, J. W. (2015) Centrosome function and assembly in animal cells. *Nat. Rev. Mol. Cell Biol.* **16**, 611–624
10. Fu, J., Hagan, I. M., and Glover, D. M. (2015) The centrosome and its duplication cycle. *Cold Spring Harb. Perspect. Biol.* **7**, a015800
11. Azimzadeh, J., and Bornens, M. (2007) Structure and duplication of the centrosom. *J. Cell Sci.* **120**, 2139–2142
12. Fong, C. S., Kim, M., Yang, T. T., Liao, J. C., and Tsou, M. F. (2014) SAS-6 assembly templated by the lumen of cartwheel-less centrioles precedes centriole duplication. *Dev. Cell* **30**, 238–245
13. Leidel, S., Delattre, M., Cerutti, L., Baumer, K., and Gonczy, P. (2005) SAS-6 defines a protein family required for centrosome duplication in C. elegans and in human cells. *Nat. Cell Biol.* **7**, 115–125
14. Strnad, P., Leidel, S., Vinogradova, T., Euteneuer, U., Khodjakov, A., and Gonczy, P. (2007) Regulated HsSAS-6 levels ensure formation of a single procentriole per centriole during the centrosome duplication cycle. *Dev. Cell* **13**, 203–213
15. Habedanck, R., Stierhof, Y. D., Wilkinson, C. J., and Nigg, E. A. (2005) The Polo kinase Plk4 functions in centriole duplication. *Nat. Cell Biol.* **7**, 1140–1146
16. Bettencourt-Dias, M., Rodrigues-Martins, A., Carpenter, L., Riparbelli, M., Lehmann, L., Gatt, M. K., *et al.* (2005) SAK/PLK4 is required for centriole duplication and flagella development. *Curr. Biol.* **15**, 2199–2207
17. Kleylein-Sohn, J., Westendorf, J., Le Clech, M., Habedanck, R., Stierhof, Y. D., and Nigg, E. A. (2007) Plk4-induced centriole biogenesis in human cells. *Dev. Cell* **13**, 190–202
18. Xu, X., Huang, S., Zhang, B., Huang, F., Chi, W., Fu, J., *et al.* (2017) DNA replication licensing factor Cdc6 and Plk4 kinase antagonistically regulate centrosome duplication *via* Sas-6. *Nat. Commun.* **8**, 15164
19. Cizmecioglu, O., Arnold, M., Bahtz, R., Settele, F., Ehret, L., Haselmann-Weiss, U., *et al.* (2010) Cep152 acts as a scaffold for recruitment of Plk4 and CPAP to the centrosome. *J. Cell Biol.* **191**, 731–739
20. Dzhindzhev, N. S., Yu, Q. D., Weiskopf, K., Tzolovsky, G., Cunha-Ferreira, I., Riparbelli, M., *et al.* (2010) Asterless is a scaffold for the onset of centriole assembly. *Nature* **467**, 714–718
21. Hatch, E. M., Kulukian, A., Holland, A. J., Cleveland, D. W., and Stearns, T. (2010) Cep152 interacts with Plk4 and is required for centriole duplication. *J. Cell Biol.* **191**, 721–729
22. Kim, T. S., Park, J. E., Shukla, A., Choi, S., Murugan, R. N., Lee, J. H., *et al.* (2013) Hierarchical recruitment of Plk4 and regulation of centriole biogenesis by two centrosomal scaffolds, Cep192 and Cep152. *Proc. Natl. Acad. Sci. U. S. A.* **110**, E4849–4857
23. Sonnen, K. F., Gabryjonczyk, A. M., Anselm, E., Stierhof, Y. D., and Nigg, E. A. (2013) Human Cep192 and Cep152 cooperate in Plk4 recruitment and centriole duplication. *J. Cell Sci.* **126**, 3223–3233
24. Chi, W., Wang, G., Xin, G., Jiang, Q., and Zhang, C. (2021) PLK4-phosphorylated NEDD1 facilitates cartwheel assembly and centriole biogenesis initiations. *J. Cell Biol.* **220**, 202002151
25. Arquint, C., Gabryjonczyk, A. M., Imseng, S., Bohm, R., Sauer, E., Hiller, S., *et al.* (2015) STIL binding to Polo-box 3 of PLK4 regulates centriole duplication. *Elife* **4**, e07888
26. Dzhindzhev, N. S., Tzolovsky, G., Lipinszki, Z., Schneider, S., Lattao, R., Fu, J., *et al.* (2014) Plk4 phosphorylates Ana2 to trigger Sas6 recruitment and procentriole formation. *Curr. Biol.* **24**, 2526–2532
27. Kratz, A. S., Barenz, F., Richter, K. T., and Hoffmann, I. (2015) Plk4-dependent phosphorylation of STIL is required for centriole duplication. *Biol. Open* **4**, 370–377
28. Moyer, T. C., Clutario, K. M., Lambrus, B. G., Daggubati, V., and Holland, A. J. (2015) Binding of STIL to Plk4 activates kinase activity to promote centriole assembly. *J. Cell Biol.* **209**, 863–878
29. Ohta, M., Ashikawa, T., Nozaki, Y., Kozuka-Hata, H., Goto, H., Inagaki, M., *et al.* (2014) Direct interaction of Plk4 with STIL ensures formation of a single procentriole per parental centriole. *Nat. Commun.* **5**, 5267
30. Keller, D., Orpinell, M., Olivier, N., Wachsmuth, M., Mahen, R., Wyss, R., *et al.* (2014) Mechanisms of HsSAS-6 assembly promoting centriole formation in human cells. *J. Cell Biol.* **204**, 697–712
31. Guichard, P., Desfosses, A., Maheshwari, A., Hachet, V., Dietrich, C., Brune, A., *et al.* (2012) Cartwheel architecture of Trichonympha basal body. *Science* **337**, 553
32. Hilbert, M., Noga, A., Frey, D., Hamel, V., Guichard, P., Kraatz, S. H., *et al.* (2016) SAS-6 engineering reveals interdependence between cartwheel and microtubules in determining centriole architecture. *Nat. Cell Biol.* **18**, 393–403

33. Kitagawa, D., Vakonakis, I., Olieric, N., Hilbert, M., Keller, D., Olieric, V., *et al.* (2011) Structural basis of the 9-fold symmetry of centrioles. *Cell* **144**, 364–375
34. Nakazawa, Y., Hiraki, M., Kamiya, R., and Hirono, M. (2007) SAS-6 is a cartwheel protein that establishes the 9-fold symmetry of the centriole. *Curr. Biol.* **17**, 2169–2174
35. van Breugel, M., Hirono, M., Andreeva, A., Yanagisawa, H. A., Yamaguchi, S., Nakazawa, Y., *et al.* (2011) Structures of SAS-6 suggest its organization in centrioles. *Science* **331**, 1196–1199
36. van Breugel, M., Wilcken, R., McLaughlin, S. H., Rutherford, T. J., and Johnson, C. M. (2014) Structure of the SAS-6 cartwheel hub from Leishmania major. *Elife* **3**, e01812
37. Yoshiba, S., Tsuchiya, Y., Ohta, M., Gupta, A., Shiratsuchi, G., Nozaki, Y., *et al.* (2019) HsSAS-6-dependent cartwheel assembly ensures stabilization of centriole intermediates. *J. Cell Sci.* **132**, jcs217521
38. Arquint, C., Sonnen, K. F., Stierhof, Y. D., and Nigg, E. A. (2012) Cell-cycle-regulated expression of STIL controls centriole number in human cells. *J. Cell Sci.* **125**, 1342–1352
39. Tang, C. J., Lin, S. Y., Hsu, W. B., Lin, Y. N., Wu, C. T., Lin, Y. C., *et al.* (2011) The human microcephaly protein STIL interacts with CPAP and is required for procentriole formation. *EMBO J.* **30**, 4790–4804
40. Vulprecht, J., David, A., Tibelius, A., Castiel, A., Konotop, G., Liu, F., *et al.* (2012) STIL is required for centriole duplication in human cells. *J. Cell Sci.* **125**, 1353–1362
41. Cabral, G., Sans, S. S., Cowan, C. R., and Dammermann, A. (2013) Multiple mechanisms contribute to centriole separation in C. elegans. *Curr. Biol.* **23**, 1380–1387
42. Pagan, J. K., Marzio, A., Jones, M. J., Saraf, A., Jallepalli, P. V., Florens, L., *et al.* (2015) Degradation of Cep68 and PCNT cleavage mediate Cep215 removal from the PCM to allow centriole separation, disengagement and licensing. *Nat. Cell Biol.* **17**, 31–43
43. Sluder, G. (2013) Centriole engagement: it's not just cohesin any more. *Curr. Biol.* **23**, R659–660
44. Lee, K., and Rhee, K. (2012) Separase-dependent cleavage of pericentrin B is necessary and sufficient for centriole disengagement during mitosis. *Cell Cycle* **11**, 2476–2485
45. Matsuo, K., Ohsumi, K., Iwabuchi, M., Kawamata, T., Ono, Y., and Takahashi, M. (2012) Kendrin is a novel substrate for separase involved in the licensing of centriole duplication. *Curr. Biol.* **22**, 915–921
46. Kim, J., Lee, K., and Rhee, K. (2015) PLK1 regulation of PCNT cleavage ensures fidelity of centriole separation during mitotic exit. *Nat. Commun.* **6**, 10076
47. Holt, L. J., Tuch, B. B., Villen, J., Johnson, A. D., Gygi, S. P., and Morgan, D. O. (2009) Global analysis of Cdk1 substrate phosphorylation sites provides insights into evolution. *Science* **325**, 1682–1686
48. Arquint, C., and Nigg, E. A. (2014) STIL microcephaly mutations interfere with APC/C-mediated degradation and cause centriole amplification. *Curr. Biol.* **24**, 351–360
49. Hatano, T., and Sluder, G. (2012) The interrelationship between APC/C and Plk1 activities in centriole disengagement. *Biol. Open* **1**, 1153–1160
50. Nakamura, A., Arai, H., and Fujita, N. (2009) Centrosomal Aki1 and cohesin function in separase-regulated centriole disengagement. *J. Cell Biol.* **187**, 607–614
51. Thein, K. H., Kleylein-Sohn, J., Nigg, E. A., and Gruneberg, U. (2007) Astrin is required for the maintenance of sister chromatid cohesion and centrosome integrity. *J. Cell Biol.* **178**, 345–354
52. Tsou, M. F., Wang, W. J., George, K. A., Uryu, K., Stearns, T., and Jallepalli, P. V. (2009) Polo kinase and separase regulate the mitotic licensing of centriole duplication in human cells. *Dev. Cell* **17**, 344–354
53. Schockel, L., Mockel, M., Mayer, B., Boos, D., and Stemmann, O. (2011) Cleavage of cohesin rings coordinates the separation of centrioles and chromatids. *Nat. Cell Biol.* **13**, 966–972
54. Ito, K. K., Watanabe, K., Ishida, H., Matsuhashi, K., Chinen, T., Hata, S., *et al.* (2021) Cep57 and Cep57L1 maintain centriole engagement in interphase to ensure centriole duplication cycle. *J. Cell Biol.* **220**, 202005153
55. Watanabe, K., Takao, D., Ito, K. K., Takahashi, M., and Kitagawa, D. (2019) The Cep57-pericentrin module organizes PCM expansion and centriole engagement. *Nat. Commun.* **10**, 931
56. Zhang, X., Chen, Q., Feng, J., Hou, J., Yang, F., Liu, J., *et al.* (2009) Sequential phosphorylation of Nedd1 by Cdk1 and Plk1 is required for targeting of the gammaTuRC to the centrosome. *J. Cell Sci* **122**, 2240–2251
57. Zitouni, S., Francia, M. E., Leal, F., Montenegro Gouveia, S., Nabais, C., Duarte, P., *et al.* (2016) CDK1 prevents unscheduled PLK4-STIL complex assembly in centriole biogenesis. *Curr. Biol.* **26**, 1127–1137